

## THERMAL TESTING OF RETROFIT AC LEDs

András POPPE<sup>1,2</sup>, Gábor FARKAS<sup>2</sup>, Tamás TEMESVÖLGYI<sup>1,2</sup>,  
Balázs KATONA<sup>2</sup>, Gábor MOLNÁR<sup>2</sup>, Csaba BARNÁ<sup>2</sup>

<sup>1</sup>Budapest University of Technology & Economics, Dept. of Electron Devices, Budapest, Hungary,

<sup>2</sup>Mentor Graphics MicReD Division, Budapest, Hungary

andras\_poppe@mentor.com, poppe@eet.bme.hu

### Abstract

In this paper we aim at highlighting different aspects of thermal testing of AC LEDs, especially of retrofit LED lamps which are directly driven from the AC mains supply. The main focus is the concept of thermal impedance applied for AC driven LEDs and the AC heating power. The paper gives an overview of the different representations of the thermal impedance then provides estimates of the AC power of LEDs for one of the extreme cases (ideal AC voltage generator driven situation) together with spectra of harmonics of the AC heating power. Definitions and test procedures for the AC thermal impedance of LEDs are suggested along with test environments for AC LED modules as well as for complete retrofit LED lamps. The basic concept of our proposed measurement method is presented through real measurement examples.

Keywords: AC LEDs, thermal impedance of LEDs, heating power of LEDs, combined thermal and photometric/radiometric measurement of LEDs

### 1 Introduction

There is a continuous development in high power LEDs, both in terms of efficacy and in terms of applications. LED lighting applications can be driven either by a constant current LED-driver circuit or "directly" by AC power, in different configurations [1], [2], [3]. Due to overall energy efficiency considerations different retrofit LED applications have appeared even at households for indoor use, composed of several LED chips connected in series. The DC and AC powering solutions for indoor LED lighting applications seem to continue their competition.

The advantage of the DC current drive is easy dimming. In AC driven LEDs the driver electronics is simplified to a small integrated ballast, sometimes a serial resistor only, sometimes a component of reactive nature (see Figure 1).

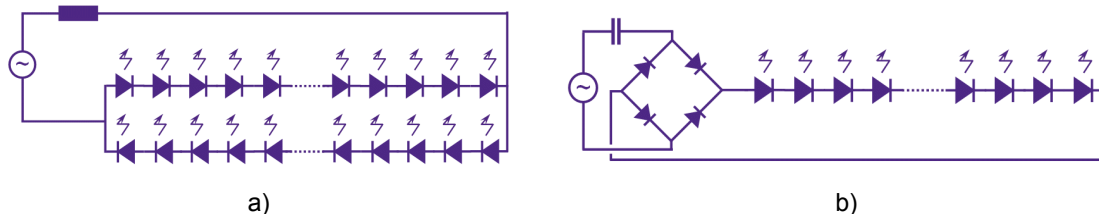


**Figure 1.** Electrical schemes of AC driven LED lamps: a) series of anti-parallel connected LEDs and resistive ballast b) capacitive ballast and bridge rectifier

Regardless whether DC or direct AC powering is used proper thermal design of a LED lighting application is a must since the light output and life-time of LEDs drop with increasing temperature. At constant DC powering LEDs dissipate steady power. This results in a steady junction temperature after a relatively short heating transient. Due to basically 1D heat spreading in LED components a single *thermal resistance* value is mostly sufficient for designing a cooling solution.

In case of AC driven LEDs the sinusoidal AC mains voltage results in a periodic waveform of the actual heating power, after an initial, transitional period while heating up the LED junctions. Once the shapes of the waveforms of the heating power and the junction temperature do not change any more we can say that the AC LED is in a *stationary state*. As our systems are nearly linear in the thermal domain the thermally stationary situation can be treated similarly to the small signal AC operation of linear electronic circuits.

Regarding thermal testing of DC driven LEDs there seems to develop an agreement among experts [4], that testing procedures can be based on existing standards like the JEDEC JESD51-1 electrical test method [5] combined with CIE 127-2007 recommendations of total flux measurement [6] – as it is described in detail in a recent publication [7]. The main point is, that for obtaining *real thermal*

resistance (or thermal impedance) of LEDs the radiant flux needs also to be considered. So, a suggested test setup is measuring DC driven LEDs on a cold-plate attached to an integrating sphere. This setup would match the requirements for the *junction-to-case* thermal measurements. For AC driven retrofit LED lamps however, *natural convection* is the usual operational environment, therefore it seems, a standardized natural convection test environment would be required and another thermal metric, junction-to-ambient AC thermal impedance would make sense. The issues we discuss in this paper include:

- application of the usual thermal impedance concept,
- detailed analysis of the AC heating power of AC LEDs,
- possible definitions of a single number as a thermal metric to characterize the thermal performance of AC driven LEDs for a given mains frequency,
- meaningful test procedures and
- appropriate test environment.

## 2 Different Representations of the Thermal Impedance

The thermal impedance of the *junction-to-ambient* heat-flow path of an LED package is a unique property of the package. It can be represented in different forms which are equivalent in terms of information content but in practical applications they can be used for different purposes. For example the steady-state thermal resistance can be read from the measured real  $Z_{th}$  curve of the LED. Figure 2 shows this curve for a 10W white LED attached to an MCPCB and measured on a cold-plate attached to an integrating sphere ( $I_F=350\text{mA}$ ,  $T_{CP}=25^\circ\text{C}$ ).

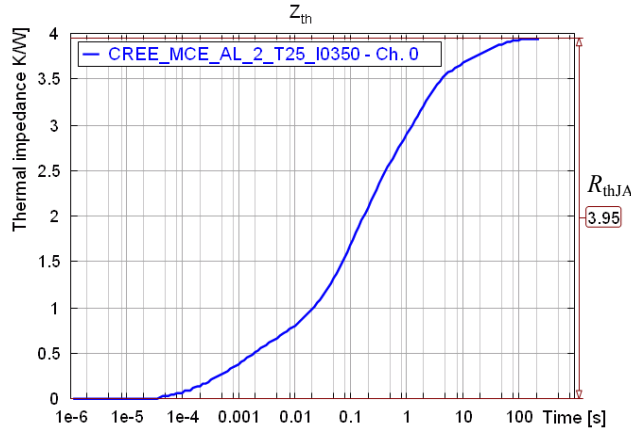


**Figure 2.** Thermal impedance curve of a 10 W white LED driven by a DC forward current of 350 mA, measured by the JESD51-1 [5] electrical test method. Highest time resolution: 1  $\mu\text{s}$ , temperature resolution: 0.01 $^\circ\text{C}$ ; total radiant flux considered in the heating power.

### 2.1 Thermal impedance curves

The classical representation of the thermal impedance of a semiconductor component is the  $Z_{th}$  curve (Figure 2), which is the junction temperature response in time to a unit-height heating power step (unit-step response), drawn in logarithmic time-scale.

Thermal impedance curves of semiconductor packages are classically measured with thermal transient test equipment, using the so called electrical test method as defined in the JEDEC JESD51-1 document [5]. (In case of LEDs the emitted total radiant flux also has to be considered in the heating power when measuring the thermal impedance [4], [7].) This curve yields rough estimates on the junction-to-ambient heat-flow path of a packaged semiconductor chip. Usually the steady-state value, the thermal resistance is used both as a thermal metric and as input for system level design of thermal management. The temperature response to any  $P_{dissDC}$  steady-state power can be calculated as

$$T_j = R_{thJA} \cdot P_{dissDC} + T_{amb} \quad (1)$$

where  $R_{thJA}$  denotes the junction to ambient thermal resistance i.e. the final value of a  $Z_{th}$  curve (see Figure 2) and  $T_{amb}$  is the ambient temperature.

## 2.2 Structure functions and network model representation

*Cumulative structure functions* identified from real  $Z_{th}$  curves are alternative representations of the thermal impedance. (They are graphical representations of a detailed ladder network model of the thermal impedance.) For practical applications a step-wise approximation of the cumulative structure function results in a compact thermal model of the measured thermal impedance in the form of a reduced ladder network of a few stages such as shown in Figure 3b.

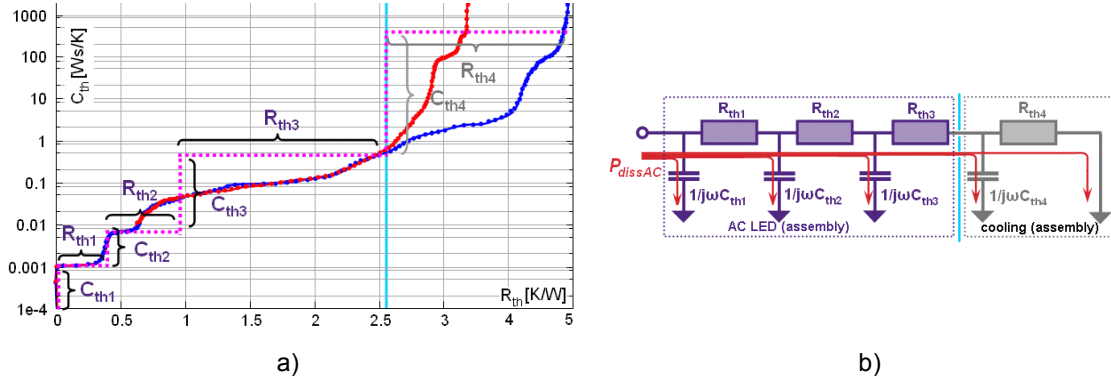


**Figure 3.** Different models calculated from the  $Z_{th}$  curve of Figure 1: a) Cumulative structure functions with different TIM layer at the package case surface (vertical line after 2.5 K/W); b) Thermal RC network model of the LED package and of its thermal environment, values can be taken from a).

In case of packages possessing an essentially one dimensional heat-flow (like almost all power LED packages) *structure functions* provide a means of distinguishing between the different sections of the heat-flow path. This is an important feature if we are interested only in the thermal impedance of the LED package itself and we want to subtract the contribution of the environment (e.g. the thermal interface material or the heat-sink) from the total junction-to-ambient thermal resistance. For example, the so called dual interface method [8] applies two different qualities of thermal interface at the case surface of the package.

In AC conditions the frequency dependent temperature response is of interest. Using the frequency domain description of the thermal impedance the temperature can be calculated as:

$$T_j(\omega) = Z_{th}(\omega) \cdot P_{dissAC}(\omega) \quad (2)$$

where  $\omega$  is (angular) frequency and  $P_{dissAC}$  is the AC power dissipation. As shown later, obtaining  $P_{dissAC}$  is not trivial. The dynamic compact network model representation of the thermal impedance can be used for such calculations. Eq. (3) provides the frequency domain representation of the thermal impedance in analytic form; calculated for the network model of Figure 3b:

$$Z_{th}(\omega) = \frac{1}{j\omega C_{th1}} \times \left\{ R_{th1} + \frac{1}{j\omega C_{th2}} \times \left( R_{th2} + \left[ \frac{1}{j\omega C_{th3}} \times (R_{th3} + Z_{hs}) \right] \right) \right\} \quad (3)$$

For the element values notation of Figure 3b was used.  $Z_{hs}$  denotes the thermal impedance of the TIM and the heat-sink (modeled by  $R_{th4}$  and  $C_{th4}$  in case of the present example) and the  $\times$  symbol represents the "re-plus" operation (i.e. resulting in the net impedance/resistance of two parallel branches). Eq. (3) suggests that at higher frequency the thermal impedance shrinks since the terms  $1/j\omega C_{th}$  tend to 0. (We described earlier structure function based compact thermal models for cooling assemblies in [9].)

Due to the assumed linearity of the thermal system a  $P_{dissAC}(t) = P_{max} \cdot \sin(\omega t)$  sinusoidal time function of the dissipated power would result in a junction temperature also having sinusoidal waveform:

$$T_{JAC}(t) = T_{Jmax} \cdot \sin(\omega t - \varphi), \quad T_{Jmax} = |Z_{th}(\omega)| \cdot P_{max} \quad (4)$$

This means assuming constant amplitude of the power the amplitude of the junction temperature changes with the frequency since the value of  $|Z_{th}(\omega)|$  vanishes with increasing frequency as it already concludes from Eq. (3). This also suggests that the AC thermal impedance (yet to be exactly defined in a subsequent section) of the same AC LED lamp would be different when operated from a 50 Hz mains or from a 60 Hz mains (see also Figure 4). In reality sinusoid power change does not occur. However, periodic power waveforms have a Fourier decomposition of harmonic changes around a

mean (DC) power level. Eq. (4) describes any of these harmonics. The relationship between a periodic dissipation function and its harmonic components is

$$P_{\text{dissAC}}(t) = \sum_{n=0}^{\pm\infty} P_n \cdot e^{jn\omega_0 t} \quad (5)$$

where the complex number  $P_n$  denotes the Fourier-coefficient of the  $n$ -th harmonic of the  $P_{\text{dissAC}}(t)$  "signal". Introducing the notation of  $Z_{\text{th}-n} = Z_{\text{th}}(n\omega_0)$  – where  $\omega_0$  refers to the frequency of the base harmonic – the Fourier series expansion of real  $T_{\text{JAC}}(t)$  time functions can be expressed as

$$T_{\text{JAC}}(t) = \sum_{n=0}^{\pm\infty} Z_{\text{th}-n} \cdot P_n \cdot e^{jn\omega_0 t} \quad (6)$$

### 2.3 Complex locus

The  $Z_{\text{th}}(\omega)$  frequency domain representation of the thermal impedance can be mathematically derived from the measured  $Z_{\text{th}}$  thermal impedance as follows:

$$Z_{\text{th}}(\omega) = \int_0^{\infty} a(t)e^{-j\omega t} dt \quad (7)$$

where  $a(t)$  is the unit power-step temperature response function, (junction temperature transient normalized to  $P_{\text{dissDC}}$ ) and  $\omega$  is the angular frequency of the excitation. The resulting  $Z_{\text{th}}(\omega)$  complex thermal impedance function can be visualized in a *Bode diagram* or as complex locus.

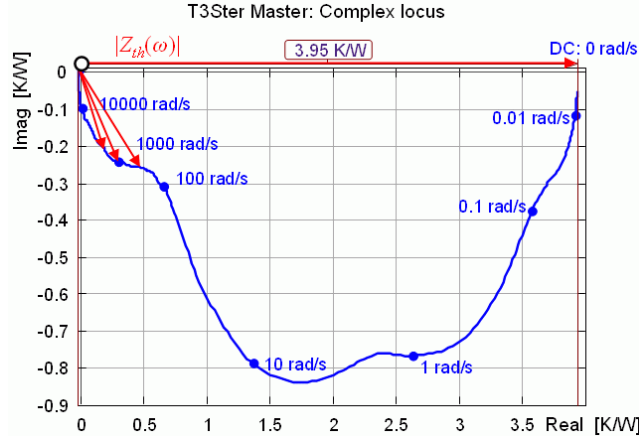


**Figure 4.** Complex locus of a 10 W white LED. Harmonic components corresponding to 0 Hz, 100 Hz, 200 Hz, 300 Hz are shown.

Figure 4 shows the behavior of a 10 W white LED switched down from steady 350 mA to a small measurement current (10 mA). The 0 frequency value is the thermal resistance defined by Eq. (1). If the mains voltage is e.g. 50 Hz then the power will have 100 Hz base frequency and so harmonics of 200 Hz, 300 Hz etc will also appear (see later). The corresponding angular frequencies of interest in Figure 4 will be accordingly 628 rad/s, 1258 rad/s, 1885 rad/s etc. The absolute value of the impedance at any frequency is the length of the vector pointing from the origin to the given frequency point on the  $Z_{\text{th}}(\omega)$  locus (arrows in Figure 4). These vectors are always shorter than the DC value of the thermal impedance ( $R_{\text{thJA}}$ ). This is also implied by the compact network model of the thermal impedance shown in Figure 3b.

## 3 The AC heating power of LEDs

### 3.1 Analytical results for the AC dissipation of LEDs

First we present an extreme case by analytical formulae: we apply a sinusoid voltage source and use the simplest LED device model, assuming the I-V characteristic:

$$I_{\text{LED}} = I_{\text{ideal}}(V_F) + I_{\text{rec}}(V_F) \quad (8)$$

where  $I_{\text{ideal}}$  corresponds to the classic diode current detailed below,  $I_{\text{rec}}$  denotes the recombination current which is associated with light emission; therefore, when considering the heating power of an LED, this portion of the forward current will not be taken into account. If the series electrical resistance

of the LED is negligible, the  $V_F$  forward voltage across the LED's pn-junction is equal to the generator voltage:  $V_F = V_{AC}$ . Eq. (8) is true for the forward characteristics of the diode only. However, most AC LEDs utilize both halves of the sine wave with appropriate circuitry (Figure 1), this way Eq. (8) can be used for AC voltage, although  $I_{LED}$  flows in different diodes in the two halves. With  $V_{AC} = V_{MAX} \cdot \sin(\omega t)$  voltage change the current of the LED can be described as:

$$I_{LED}(t) = I_0 \cdot [\exp(V_{MAX} \cdot \sin(\omega t) / mV_T) - 1] + I_{rec}(V_{MAX} \cdot \sin(\omega t)) \quad (9)$$

where  $I_0$  is the current constant of the ideal diode characteristic (saturation current),  $V_T \approx kT/q$  is the thermal voltage and  $m$  is the so called ideality factor ( $m \approx 1.2$ ). The AC generator voltage is also substituted into the  $I_{rec}(V)$  function representing the light emission. The dissipated AC power of the LED is determined by the AC voltage drop across the LED (the AC generator voltage) and the current not associated with light generation:

$$P_{dissAC}(t) = I_0 [\exp(V_{MAX} \cdot \sin(\omega t) / mV_T) - 1] \cdot V_{MAX} \cdot \sin(\omega t) \quad (10)$$

Substituting the  $\exp(V_{MAX} \cdot \sin(\omega t) / mV_T)$  term with the Taylor-series approximation of the exponential function and performing the multiplication with  $V_{MAX} \cdot \sin(\omega t)$  in Eq. (10):

$$P_{dissAC}(t) = V_{MAX}^2 \cdot \frac{I_0}{mV_T} \cdot \frac{1}{1!} \sin^2(\omega t) + V_{MAX}^3 \cdot \frac{I_0}{(mV_T)^2} \cdot \frac{1}{2!} \sin^3(\omega t) + V_{MAX}^4 \cdot \frac{I_0}{(mV_T)^3} \cdot \frac{1}{3!} \sin^4(\omega t) + \dots \quad (11)$$

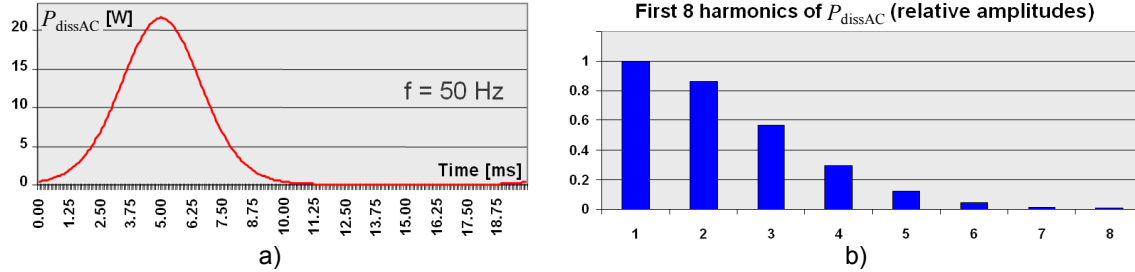


**Figure 5.** AC dissipation waveform (1 period) for a purely AC voltage generator driven LED according to Eq. (10) and the relative amplitudes of its first eight harmonics – see Eq. (5).

We can see that due to the nonlinearity of the LEDs' I-V characteristics, higher harmonics of the base frequency of the AC generator will appear in the dissipation. The even harmonics add to the DC level of the dissipated power, since  $\sin^2(\alpha) = [1 - \cos(2\alpha)]/2$ ,  $\sin^4(\alpha) = [3 - 4\cos(2\alpha) + \cos(4\alpha)]/8$ , etc. The first harmonic represents a  $1/2$ , the fourth a  $3/8 \times 1/2$  part of the DC level and so on.

Since  $\sin^3(\alpha) = [3\sin(\alpha) - \sin(3\alpha)]/4$  the odd harmonics cause the base harmonics to appear in the power change but at a lower factor only. The actual time function of  $P_{dissAC}$  as per Eq. (10) for a single period of the AC supply voltage of the form of  $V_{MAX} \cdot \sin(\omega t)$  together with the relative amplitudes of its first eight harmonics is shown in Figure 5. The harmonics shown in Figure 5b represent the first 8  $P_n$  values from the sum of Eq. (5). Calculations for the AC current driven case can be found in [10].

### 3.2 Examples for the measurement of the AC dissipation of LEDs

First we carried out experiments which can be repeated anywhere using general laboratory equipment. We investigated an SSC Acriche AC LED aimed at 230V AC mains power [11].

The LED and a 1.3k $\Omega$  series resistor ballast (as per the scheme of Figure 1a) were factory mounted on an MCPCB. The LED was attached to a water cooled cold-plate (Figure 6) and directly connected to the 230 V / 50 Hz mains.

Both the AC current (on the ballast) and the voltage of the LED were monitored in the LED's stationary state by a digital oscilloscope (Agilent DS05032A). The waveform of the electrical power was calculated by the oscilloscope itself from the captured current and voltage (Figure 7a). The small arrows with numbers 1,2,3 show the zero level of the voltage, current, power signal on the scope display, respectively. We can clearly see that all waveforms are significantly distorted compared to sinusoidal shape proving that the powering is a complex periodic waveform of high harmonic content.

The harmonic analysis results performed by the oscilloscope software for the current of the LED under test are shown in Figure 7b.

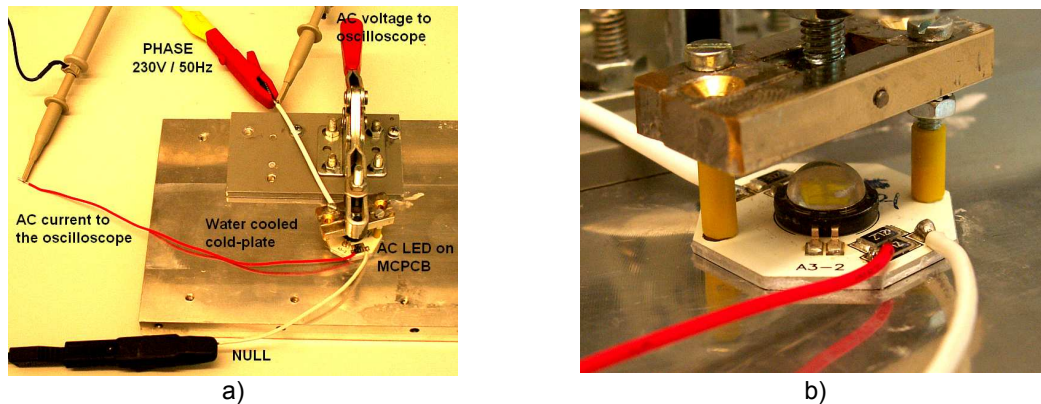


**Figure 6.** Measurement of an 230V AC LED: a) the measurement setup, b) close-up view of the LED under test.

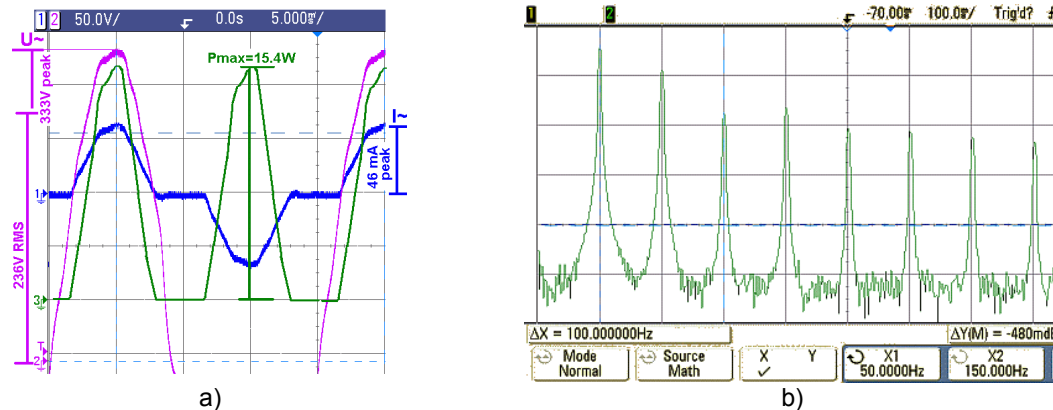


**Figure 7.** Measurement of an 230 V AC LED: a) voltage, current and electrical power waveforms captured by a digital oscilloscope, b) harmonic amplitudes of the current through the LED line.

Note, that in this example the AC voltage was obtained from the AC mains outlet – already having significant harmonic distortion. In order to obtain repeatable results, measurements should be carried out using an AC signal with no distortion.

In the next, more complex trial we attempted a correct measurement of the emitted light as function of the time. As suggested earlier for DC driven LEDs [4], [7], the AC radiant flux was measured in an integrating sphere [12]. We mounted an experimental 6x8 LED array (48 LEDs) on the temperature regulated device holder of an integrating sphere.

The chain of LEDs with 10 k $\Omega$  ballast produced approximately 215V at 5 mA and 225 V at 10 mA DC (at room temperature) with nearly 100 mV/K temperature sensitivity.

The built in photodetector in the sphere is an integrating type for high accuracy and low noise; and as such it provides an average value of the radiant flux of AC LEDs. Therefore a fast reverse biased photodiode was also inserted into the sphere. We calibrated its current in DC mode to the standard detector, this way the AC signal of the photodiode corresponded to the actual time function of the radiant flux. All waveforms were downloaded from the digital oscilloscope in text format and further processed in Excel. The results of this measurement are shown in Figure 8.

## 4 Possibilities for the measurement of the AC thermal impedance of LEDs

### 4.1 Direct adaptation of the JEDEC JESD51-1 electrical test method for AC driven heating

To assure accuracy and repeatability of results, direct measurement of the real AC thermal impedance of LEDs should be performed by care. The period of the mains voltage (20ms/16.66ms) is much longer than the smallest thermal time-constants of usual LEDs – about 20% of the thermal change of a LED occurs in this time interval.

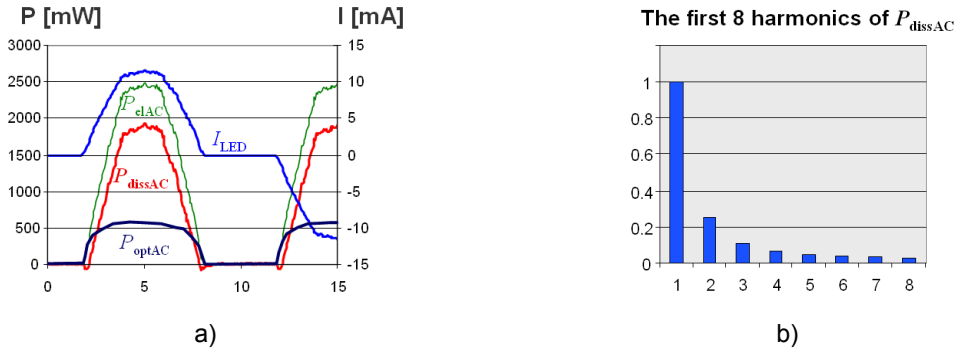


**Figure 8.** Measurement of the power waveforms of an AC LED: a) AC current, electrical power, AC radiant and AC dissipation waveforms measured at 50 Hz, b) relative amplitudes of the first eight harmonics of the AC heating power

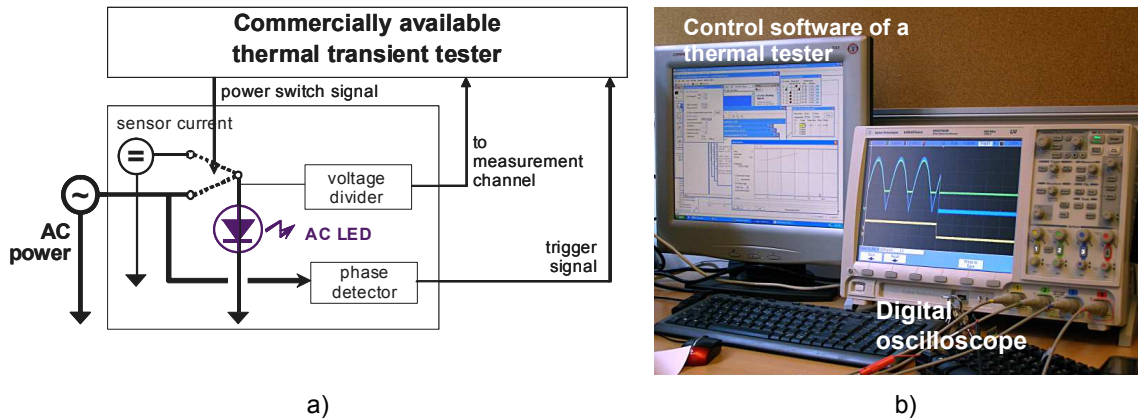


**Figure 9.** Measurement of AC LEDs using commercially available thermal test equipment: a) schematic of the measurement setup following the basic principles of the JEDEC JESD51-1 electrical test method, b) display of the measurement software of the thermal test equipment and a digital oscilloscope attached to the device under test.

#### 4 Possibilities for the measurement of the AC thermal impedance of LEDs

##### 4.1 Direct adaptation of the JEDEC JESD51-1 electrical test method for AC driven heating

To assure accuracy and repeatability of results, direct measurement of the real AC thermal impedance of LEDs should be performed by care. The period of the mains voltage (20ms/16.66ms) is much longer than the smallest thermal time-constants of usual LEDs – about 20% of the thermal change of a LED occurs in this time interval.

Adapting the principles of the JEDEC JESD51-1 standard compliant thermal measurements, the AC LED under test must be heated by a sinusoidal AC power source. Once reaching stationary current/voltage waveforms of a constant shape the AC power can be cut off and the junction temperature drop can be measured by usual electrical test method [5]. To assure repeatability the AC power has to be switched off at a well defined phase of the AC signal. Since the maximum of the AC junction temperature occurs near the peak of the heating power, cutting off the voltage shortly after at the peak when reaching stationary state yields results corresponding to the worst case situation – 135° in Figure 11. Such a direct measurement allows the implementation of the measurement of the effective AC thermal impedance can be defined as

$$Z_{thAC} = \Delta T_J / P_{dissAC-mean} \quad (12)$$

where  $\Delta T_J$  denotes the maximal junction temperature change measured after the AC power is switched off in stationary state at a maximum of the applied AC voltage. In this approach we used a modified version of the JEDEC JESD51-1 electrical test method. Instead of a steady-state heating current a sinusoidal AC voltage source was used to heat the LED under test. In its stationary state its AC radiant power was also measured as described in the second example in section 3.2. Then the AC electrical power was suddenly switched down (within a few  $\mu s$ ) to a DC measurement current (10 mA)

and the cooling transient of the LED's pn-junction was recorded, starting with a 1  $\mu$ s time resolution. The measurement was carried out using a commercially available thermal transient test equipment [13]. The setup of the measurement is shown in Figure 9.

In order to assure reproducible measurement results, special attention was paid to the phase of the AC heating voltage at which switching to the measurement current takes place. In Figure 10 we present results for a LED where switching from the AC generator the DC measurement current took place at 0°, 45° and 90° phase of the AC voltage – resulting in a huge variation in the measured thermal impedance curve. Figure 11 presents measurement results of the measured junction temperature transients for two frequencies (50 Hz and 60 Hz) for four different phases (0°, 45°, 90° and 135°). At higher frequencies the curves go closer to the one dictated by the average power (hot gets cooler, cool gets warmer) and the spread between different phase angles of switching off the AC heating diminishes.

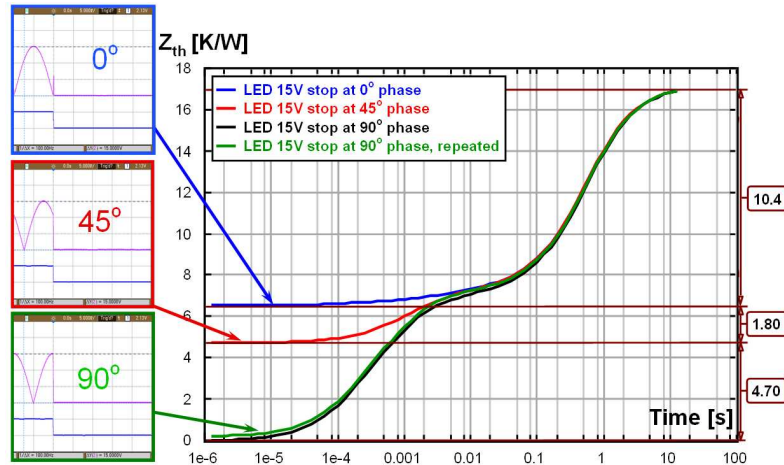


**Figure 10.** Measured of  $Z_{th}$  curves of an LED measured with a commercially available thermal transient test equipment [13] when heating was switched off at three different phases of the AC input voltage. The standard measurement setup was modified according to Figure 9a.

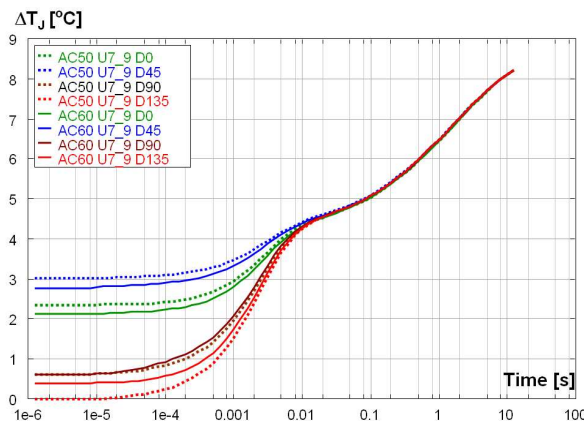


**Figure 11.** Junction temperature transients of an LED measured with a commercially available thermal transient test equipment [13] when heating was switched off at three different phases of an AC input voltage with 50 Hz and 60 Hz frequency. The standard measurement setup was modified according to Figure 9a.

#### 4.2 Existing LED test methods and calculus

The most straightforward way is using the junction to ambient *thermal impedance* which is a *unique property* of a semiconductor package. There are several ways of representing it, with well defined transformation methods among the different representations [14], [16].

Powering an AC LED by appropriately high DC voltage (up to 150..280 V – see Figure 12) one can measure the  $Z_{th}$  thermal impedance (diagrams such as shown in Figure 2) as defined in the JEDEC JESD51-1 electrical test method. Combined with CIE 127-2007 compliant total radiant flux



measurement [6] the energy of the emitted light can be considered as described e.g. in [7]. Such measurements can be performed with usual, commercially available test equipment [12], [13].

Note, that very simple ballasts like an integrated resistor (see Figure 1a and Figure 6) do not disturb usual thermal testing procedures. Capacitive AC ballasts (Figure 1b) interfere with thermal testing therefore such ballasts must be bypassed while doing thermal tests. In general, complex ballast configurations will require further investigations before attempting to define the power waveforms applied to the LEDs.

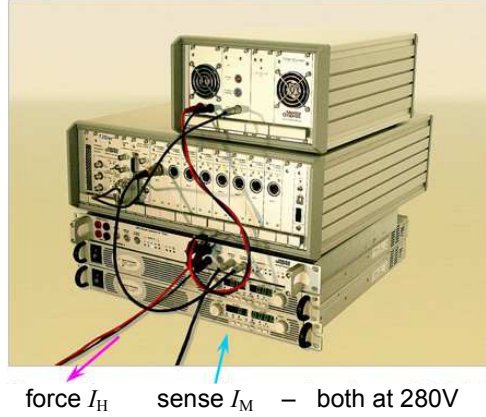


**Figure 12.** Thermal test setup using commercially available equipment capable of implementing the JEDEC JESD51-1 test method with voltage levels up to 280 V.

#### 4.2.1 Major steps

Application of mathematical procedures in obtaining simple thermal metrics of semiconductor devices first appeared in JESD51-14 [8]: the recently published transient based junction-to-case thermal resistance measurement standard for power semiconductor devices packages. The complexity of the calculus described below is much less than the apparatus used in JESD51-14, the calculations can be implemented even in a simple spreadsheet application.

The measured time domain thermal impedance curve can be transformed into frequency domain according to Eq. (7), this way one can obtain the  $Z_{th}(\omega)$  function [14], [15]. At this point we have the frequency domain model of the LED suitable for being driven by arbitrary waveforms.

As a next step, the AC voltage needed (120 V / 60 Hz or 230 V / 50 Hz) has to be applied. Once the AC LED has reached its stationary state, the waveforms of its AC voltage, current and its periodic radiant flux can be measured (see section 3.2). From these waveforms the actual  $P_{dissAC}(t)$  heating power can be calculated. With Fourier-analysis the  $P_n$  harmonic components of the LED's heating power introduced in Eq. (5) can be calculated (see e.g. Figure 8b).

Taking the values of the  $Z_{th}(\omega)$  at the harmonic frequencies of the dissipation, the waveform of the AC junction temperature can be calculated with the help of Eq. (6). Once the  $T_{JAC}(t)$  and  $P_{dissAC}(t)$  functions are known, the *effective AC thermal impedance* as a *new thermal metric* can be derived.

#### 4.2.2 Possible definitions of effective AC thermal impedance

There are several possibilities to define such a thermal metric, such as the ratio of (some proper) mean values:

$$Z_{thAC-mean} = T_{JAC-mean} / P_{dissAC-mean} \quad (13)$$

where  $T_{JAC-mean}$  and  $P_{dissAC-mean}$  values are calculated from the stationary  $T_{JAC}(t)$  and  $P_{dissAC}(t)$  functions. An other option is to use the maximal value of the stationary junction temperature waveform to obtain a single AC thermal impedance value:

$$Z_{thAC-max} = T_{JAC-max} / P_{dissAC-mean} \quad (14)$$

where  $T_{JAC-max}$  is the peak value of the junction temperature of an AC power operated LED. Note, that regardless of the definition of the *effective AC thermal impedance*, its value depends on the frequency of the applied AC power – as suggested both by Eq. (3) and Figure 4 in section 2, so depending on the mains frequency different values are expected: the AC thermal impedance at 50Hz is always larger than at 60Hz.

## 6 Conclusions

We showed that the AC thermal impedance is inherently smaller than the steady-state thermal resistance of the same LED device and it depends on the frequency. We showed that due to the non-linear nature of LEDs' I-V characteristics the AC power dissipation of LEDs will contain significant higher harmonic terms of the base frequency. We briefly described two approaches. One is based on the direct measurement the thermal impedance, but in order to assure repeatable results, synchronizing the start of the junction temperature measurement with the actual phase of the supplied AC power is a must. An alternate method is based on existing transient test methods used for thermal testing of DC current driven power LEDs and on additional calculus with which an effective AC thermal impedance of LED devices can be obtained. We suggested definitions for the effective AC thermal impedance of LEDs. We described procedures with which existing test equipment completed with additional software (capable of e.g. harmonic analysis) can be used to measure such a new thermal metric. Two alternate definitions for LEDs' AC thermal impedance were given: one is considering the mean value of the AC junction temperature, the other definition – as a worst case approach – uses the peak value of the AC junction temperature.

## Acknowledgements

The support of the Hungarian Government through the TÁMOP-4.2.1/B-09/1/KMR-2010-0002 project at the Budapest University of Technology and Economics is acknowledged. We also wish to express our thanks to prof. Vladimír Székely (BME/Mentor Graphics) and Bernie Siegal (TEA) for fruitful discussions about thermal testing of AC LEDs.

## References

- [1] H-H. YEN, H-C. KUO, W-Y. YEH, 2008, Characteristics of Single-Chip GaN-Based Alternating Current Light-Emitting Diode, *Japanese Journal of Applied Physics* Vol. 47, pp. 8808-8810
- [2] P-T. CHOU, W-Y. YEH, M-T. LIN, S-C. TAI, H-H. YEN, 2009, Development of On-chip AC LED Lighting Technology at ITRI, *Proceedings of the 2009 CIE Midterm Conference, Light and Lighting, Budapest, Hungary*
- [3] J. CHO, J. JUNG, J. H. CHAE, HYUNGKUN KIM, HYUNSOO KIM, J. W. LEE, S. YOON, C. SONE, T. JANG, Y. PARK, E. YOON, 2007, Alternating-current light emitting diodes with a diode bridge circuitry", *Japanese Journal of Applied Physics*, Vol. 46, pp 1194–1196
- [4] A. POPPE, C. J. M. LASANCE, 2009, On the Standardization of Thermal Characterization of LEDs, *Proceedings of the 25th IEEE Semiconductor Thermal Measurement and Management Symposium (SEMI-THERM'09), San Jose, USA, 15-19 March 2009*, pp. 151-158
- [5] JEDEC Standard JESD51-1, *Integrated Circuit Thermal Measurement Method - Electrical Test Method (Single Semiconductor Device)*, <http://www.jedec.org/sites/default/files/docs/jesd51-1.pdf>
- [6] CIE 2007 CIE127-2007 Technical Report, *Measurement of LEDs*
- [7] A. POPPE, G. FARKAS, G. MOLNÁR, B. KATONA, T. TEMESVÖLGYI, J. W. HE, 2010, Emerging standard for thermal testing of power LEDs and its possible implementation, *SPIE Proceedings 7784*, paper 38 (SPIE Solid State Lighting Conference, 1-5 August 2010, San Diego, USA)
- [8] JEDEC Standard JESD51-14, *Transient Dual Interface Test Method for the Measurement of the Thermal Resistance Junction-To-Case of Semiconductor Devices with Heat Flow through a Single Path*, <http://www.jedec.org/sites/default/files/docs/JESD51-14.pdf>
- [9] G. FARKAS, A. POPPE, E. KOLLÁR, P. STEHOUWER, 2003, Dynamic Compact Models of Cooling Mounts for Fast Board Level Design, *Proceedings of the 19th IEEE Semiconductor Thermal Measurement and Management Symposium (SEMI-THERM'03), San Jose, USA, 11-13 March 2003*, pp. 255-262
- [10] A. POPPE, G. FARKAS, T. TEMESVÖLGYI, B. KATONA, G. MOLNÁR, 2010, Thermal Impedance of AC LEDs, *Proceedings of the 16th International Workshop on THERMal INvestigation of ICs and Systems (THERMINIC'10), Barcelona, Spain, 6-8 October 2010*, pp. 127-132.
- [11] <http://www.seoulsemicon.com/en/product/prd/acriche.asp>
- [12] <http://www.mentor.com/products/mechanical/products/teraled>
- [13] <http://www.mentor.com/products/mechanical/products/t3ster>
- [14] V. SZÉKELY, 1997, A New Evaluation Method of Thermal Transient Measurement Results, *Microelectronics Journal*, Vol. 28. No.3., pp 277-292
- [15] V. SZÉKELY, M. RENCZ, 2000, Thermal Dynamics and the Time Constant Domain, *IEEE Transactions On Components and Packaging Technologies*, Vol. 23, No. 3. pp 687-594